

Continuous Droplet Flow Synthesis of a Near-Infrared Responsive
Push-Pull Copolymer toward Large Scale Implementation of Organic Photodetectors
Peer-reviewed author version

BECKERS, Omar; GIELEN, Sam; VERSTRAETEN, Frederik; VERSTAPPEN, Pieter;
LUTSEN, Laurence; VANDEWAL, Koen & MAES, Wouter (2020) Continuous Droplet
Flow Synthesis of a Near-Infrared Responsive Push-Pull Copolymer toward Large
Scale Implementation of Organic Photodetectors. In: *Acs Applied Polymer Materials*,
2 (11) , p. 4373 -4378.

DOI: 10.1021/acsapm.0c00998

Handle: <http://hdl.handle.net/1942/33164>

Continuous Droplet Flow Synthesis of a Near-Infrared Responsive Push-Pull Copolymer Toward Large Scale Implementation of Organic Photodetectors

Omar Beckers^{a,b}, Sam Gielen^{a,b}, Frederik Verstraeten^{a,b}, Pieter Verstappen^{a,b}, Laurence Lutsen^b,
Koen Vandewal^{a,b}, Wouter Maes^{a,b,*}

^a UHasselt – Hasselt University, Institute for Materials Research (IMO), Agoralaan 1 – Building D, 3590 Diepenbeek, Belgium

^b IMEC, Associated Lab IMOMECE, Wetenschapspark 1, 3590 Diepenbeek, Belgium

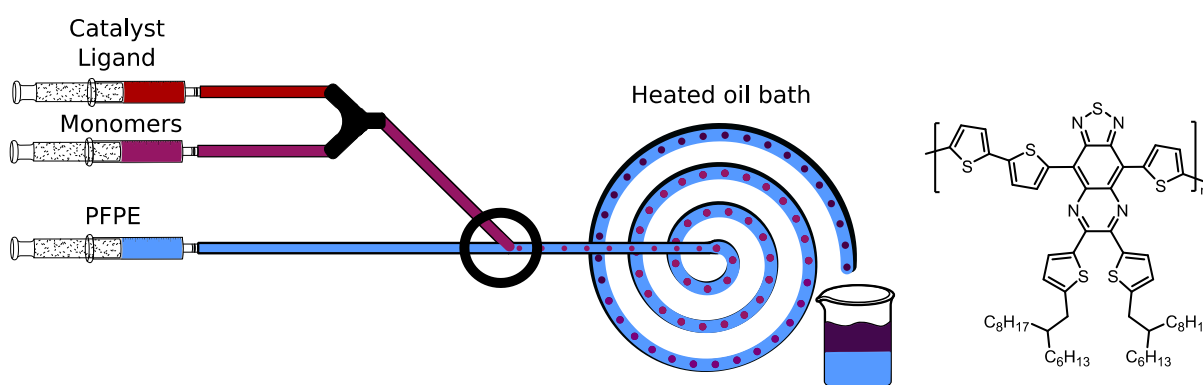
*wouter.maes@uhasselt.be

Abstract

Flow chemistry has been shown to be an excellent tool for the production of conjugated polymers. In some cases, however, this technique reaches its limits because of viscosity increases or precipitate formation. Droplet flow can provide an answer but has not been developed yet for the state-of-the-art push-pull conjugated polymers applied in many prototype organic electronic devices. In this work, a droplet flow protocol is established for a near-infrared photoactive [1,2,5]thiadiazolo[3,4-*g*]quinoxaline-based alternating copolymer, representing the first implementation of flow synthesis for organic photodetector materials. High-quality polymers are obtained, with an enhanced consistency in molar mass, dispersity, and photodetector performance.

Keywords: continuous flow synthesis · droplet flow · reproducibility · organic electronics · near-infrared photodetectors

Graphical Abstract



In recent years, continuous flow chemistry has established itself as a highly efficient and versatile tool for the development and production of tailor-made advanced polymers. High-quality materials are easily synthesized regardless of the scale, the polymerization mechanism and the type of monomers.¹ Flow chemistry has also been used by a few groups for the synthesis of conjugated polymers specifically designed for organic electronics applications such as organic photovoltaics (OPVs) and organic field-effect transistors (OFETs).²⁻⁹ Due to the fast mixing, rapid heat transfer and the ease to apply extreme conditions in flow setups, reaction times can (in general) significantly be reduced. In addition, continuous flow chemistry offers a very high control over the reaction conditions, allowing the production of advanced polymers with high reproducibility, in contrast to traditional batch chemistry. This is particularly helpful in the field of organic electronics, wherein batch-to-batch variations in the quality of (push-pull type) conjugated polymers are considered one of the main bottlenecks toward large scale implementation and commercialization.^{5,10,11} Flow chemistry also enables high-throughput screening in a straightforward way, speeding up research efforts. Moreover, large-scale material production can be foreseen in a cost-effective manner.

Despite all of the above benefits and the great potential of continuous flow chemistry, it has not been widely implemented for conjugated polymer synthesis so far. There is still a need for further refinement and dedicated research efforts to overcome important drawbacks inherent to traditional flow setups. For instance, reactor fouling can occur in case of highly viscous polymer solutions, or the formation of precipitates. This is often the case for the synthesis of conjugated (push-pull) polymers with reasonably high molar masses, affording better results in organic electronics devices.^{9,12-16} This problem can potentially be circumvented by using a droplet method in which a flow is generated by introducing a reaction mixture into a stream of an immiscible carrier fluid, which causes the formation of highly consistent low-volume droplets.¹⁷ Preferably, a carrier fluid with a large affinity for the inner wall of the tubing (e.g. a perfluorinated solvent in combination with perfluorinated-type tubing) is used, which ensures that the generated reaction droplets float through the center of the tubing without contacting the inner walls. This results in a reactor that can tolerate large increases in viscosity and the formation of small precipitates, and thus circumvents one of the main issues of traditional flow reactors. Additionally, droplet flow reactors benefit from a fast equilibration of temperature and concentration due to the small droplet size, ensuring a uniform reaction environment.¹⁷

A droplet flow procedure has previously been established for the old workhorse conjugated polymer P3HT (poly-3-hexylthiophene),⁶ but, to the best of our knowledge, no protocol for push-pull copolymers has been developed yet. Push-pull (or donor-acceptor) based copolymers are the state-of-the-art electron donor components in OPVs and organic photodetectors (OPDs), but also find their application in OFETs, organic light-emitting diodes (OLEDs) and organic electrochemical transistors (OECTs).¹⁸⁻²¹ To date, OLEDs based on small molecules are the only organic electronic devices successfully being commercialized, in television screens and smartphone displays. Polymer based OPDs might be next, as they provide a low-cost, light-weight, tunable and flexible alternative to the present generation of (inorganic) photodetectors. Nowadays, OPDs can already compete with silicon-based photodetectors in the visible region.²² However, there is a particular interest in near-infrared (NIR) OPDs because the currently used inorganic counterparts (mainly based on Ge, InGaAs or HgCdTe) have some important drawbacks, such as a limited pixel size, a high rigidity and a considerable cost.¹⁸ In previous work, we have developed push-pull copolymers based on the electron-deficient bay-annulated indigo (BAI) monomer, which allowed photodetection beyond 1000 nm in bulk heterojunction (BHJ) OPDs, with detectivities up to 10^{12} Jones.²³ Despite this good performance, the BAI synthesis is accompanied by low yields and a laborious purification, detrimental for potential upscaling. Therefore, new copolymers were designed and synthesized from the electron-poor [1,2,5]thiadiazolo[3,4-*g*]quinoxaline (TQ) precursor, which afforded photodetection up to 1.4 μm when applied in BHJ NIR-OPDs and detectivities exceeding 10^{10} Jones.²⁴ Their easy synthesis and upscaling, straightforward wavelength tunability and good performance at high wavelengths – among the highest so far for NIR-OPDs in the wavelength range beyond 1 μm – motivate further studies on these materials, for instance with respect to their production by continuous flow.

In the presented work, we show that a prototype TQ-based NIR-OPD polymer, PTTQ(HD), can efficiently be synthesized using droplet flow. The benefits of this method in terms of material production, reaction screening, reproducibility and material quality are discussed.

To illustrate the versatility of continuous droplet flow, a range of polymerization conditions and methods were tested toward the production of PTTQ(HD) (Scheme 1). For proper benchmarking, traditional batch and flow chemistry approaches were performed as well. All polymerizations were done in triplicate on a 100 mg polymer scale in chlorobenzene using $\text{Pd}_2(\text{dba})_3/\text{P}(o\text{-tol})_3$ as the catalytic system.²⁴ Regular flow experiments were conducted on a home-made setup using two syringe pumps and a heated perfluoroalkoxy (PFA) tubular reactor of 11 mL. The droplet flow setup consisted of a heated planar PFA tubular reactor of 1.13 mL, a PTFE droplet generator and also two syringe pumps (Figure 1).⁶ Prior to analysis, the polymers were purified by removal of Pd traces and consecutive Soxhlet extractions to get rid of remaining monomer and oligomer species. An overview of the applied reaction conditions and the resulting polymer molar mass properties is provided in Table 1. Details on the batch and flow synthesis procedures are provided in the Supporting Information (SI).

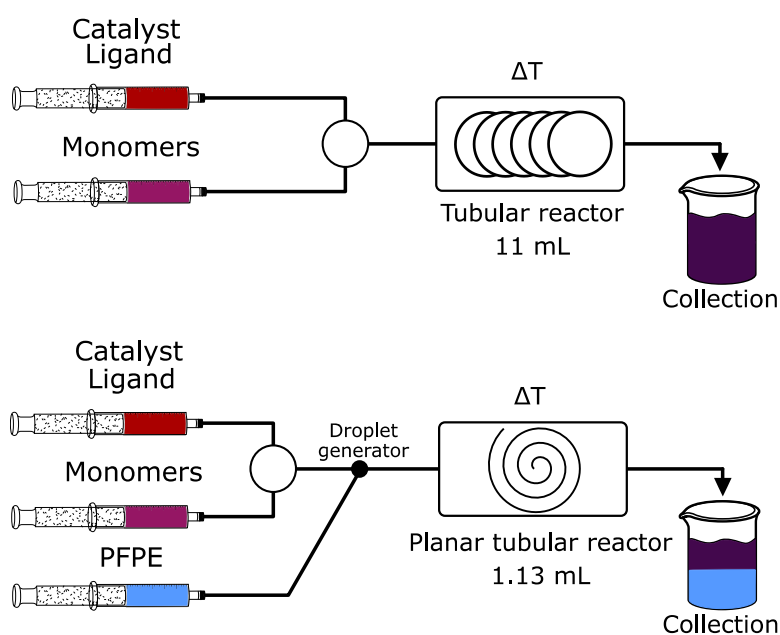
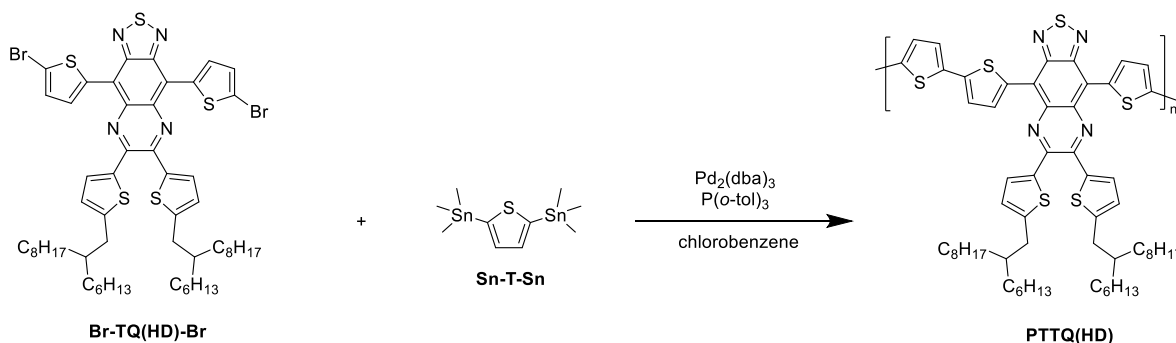


Figure 1: Continuous flow setups used in this work: regular flow (top) and droplet flow (bottom).



Scheme 1: Stille polycondensation reaction affording PTTQ(HD).

Under regular batch synthesis conditions, the PTTQ(HD) polymer (**P1**) solution becomes increasingly viscous as the polymerization progresses, resulting in large batch to batch variations due to inhomogeneity of the reaction mixture (number average molar mass (M_n) of 52.8/22.9/30.5 kg/mol for polymerization trials a/b/c, respectively; Table 1).²⁴ Typically, when conducting a transfer from batch to flow, the change in viscosity is taken into account by decreasing the concentration of the

reagent solutions.⁸ For the PTTQ(HD) synthesis by continuous flow, a concentration decrease of 50% was initially applied (from 60 to 30 mg/mL). Even under these conditions, the polymer (**P2**) occasionally coagulated on the walls of the PFA tubing and sometimes even fouled the reactor. Although the concentration decreased, a reasonably high M_n of 32.4/28.1/32.0 kg/mol was still observed, which can be attributed to the enhanced mixing and heat transfer in comparison to batch chemistry, which eventually yields more uniform products.^{25–29} To further increase reproducibility and to prevent reactor fouling, the transfer to a continuous droplet flow setup was then made.

For the first polymers prepared by droplet flow (**P3**), the monomer concentration was further decreased to 24 mg/mL. Nevertheless, similar molar masses were obtained (M_n of 35.1/44.0/29.2 kg/mol). Two follow-up experiments were executed at a lower reaction temperature of 90 °C. Polymer **P4** was synthesized using a monomer concentration of 24 mg/mL, whereas **P5** was prepared with a higher concentration of 60 mg/mL. The molar mass of polymer **P4** (M_n of 32.3/32.8/27.6 kg/mol) diminished slightly in comparison to **P3** due to the temperature drop. For **P5**, however, a sharp increase in molar mass was observed as a consequence of the increased concentration (M_n of 81.1/79.4/82.3 kg/mol). Finally, a polymer batch (**P6**) was produced using the same conditions as applied for **P5**, except for a shorter reaction time of 1 hour. As expected, a drop in molar mass was observed (M_n of 31.2/39.1/29.1 kg/mol), which confirms the ease of molar mass tunability using this setup.

Table 1: Overview of the applied reaction conditions, molar mass and dispersity values for the different PTTQ(HD) samples.

	Procedure	Temperature (°C)	Reaction time (h)	Monomer conc. (mg/mL)	M_n (kg/mol)			\mathcal{D}		
					a^\dagger	b	c	a	b	c
P1	Batch	120	18	60	52.8	22.9	30.5	2.7	2.2	1.9
P2	Regular flow	120	2.5	30	32.4	28.1	32	1.7	2.3	2.2
P3	Droplet flow	120	2.5	24	35.1	44.0	29.2	1.8	1.9	1.7
P4	Droplet flow	90	2.5	24	32.3	32.8	27.6	2.0	1.9	2.0
P5	Droplet flow	90	2.5	60	81.1	79.4	82.3	1.5	1.6	1.7
P6	Droplet flow	90	1	60	31.2	39.1	29.1	2.1	1.9	2.5

[†] All reported values are obtained after successive Soxhlet extractions. a, b and c refer to the separate batches prepared under all reaction conditions. No significant variations in conversion were observed, with isolated yields of purified polymers between 80 and 90%. Figure S2 provides a visualization of molar mass and dispersity trends.

On average, higher molar masses are (more consistently) observed for the flow experiments (Table 1), certainly when using the same concentration. Batch chemistry is always disadvantageous in terms of mixing, heat transfer and precise control as compared to continuous flow chemistry, resulting in less reproducibility.¹ On the other hand, regular flow chemistry suffers from diffusion at the head of the injection slug since the reaction mixture comes into contact with pure solvent. Diffusion decreases the concentration at the injection head, resulting in shorter polymer chains due to a decrease in reaction rate, but it also creates a broad residence time distribution (RTD).⁹ In contrast, for droplet flow, a narrow RTD is expected due to the confined nature of the droplets. This leads to a high consistency in molar mass and dispersity (\mathcal{D}), which is an essential aspect in the quest to reduce batch-to-batch variations.³⁰ Another important observation is the narrow \mathcal{D} and high molar mass for the polymers in the **P5** series, which can be attributed to an increased polymerization rate. This is an essential asset of droplet flow since these high concentrations can not be attained in regular flow reactors.

For all further material and device analysis, data for the first two batches for each polymerization protocol (a and b; see Table 1) were used to simplify comparison. Only minor differences were observed in the UV-VIS-NIR absorption spectra of the different polymer samples (Figure 2). In chloroform solution, the polymers have a near-identical absorption profile. Batch polymer **P1_b** shows a slight blue-shift as a result of the presence of low molar mass fractions, which can clearly be seen in the gel permeation chromatography (GPC) profiles (Figure 3 and S3). This effect is more pronounced in film, where the differences are in general somewhat larger, which can be attributed to variations in polymer stacking tendency. Although polymer **P1_a** also shows strong tailing at the low molar mass side

in the chromatogram (Figure 3), this is not apparent in the absorption spectra. Since UV-Vis-NIR spectroscopy is not ideally suited to reveal structural differences in the chemical composition of the polymer backbone, the materials were also analyzed by MALDI-ToF mass spectrometry (see Figure S4 and S5). Homocoupling defects can be identified in all mass spectra, as indicated by the imbalance between the donor (thiophene) and acceptor (thiadiazoloquinoline) building blocks (Figure S5). Such structural defects are known to influence the device metrics of organic electronic devices.¹¹ However, the MALDI-ToF mass spectra do not indicate significant structural differences between the polymers prepared via the different polymerization conditions described above. The applied variation in synthesis conditions thus mainly affects the molar mass (distribution).

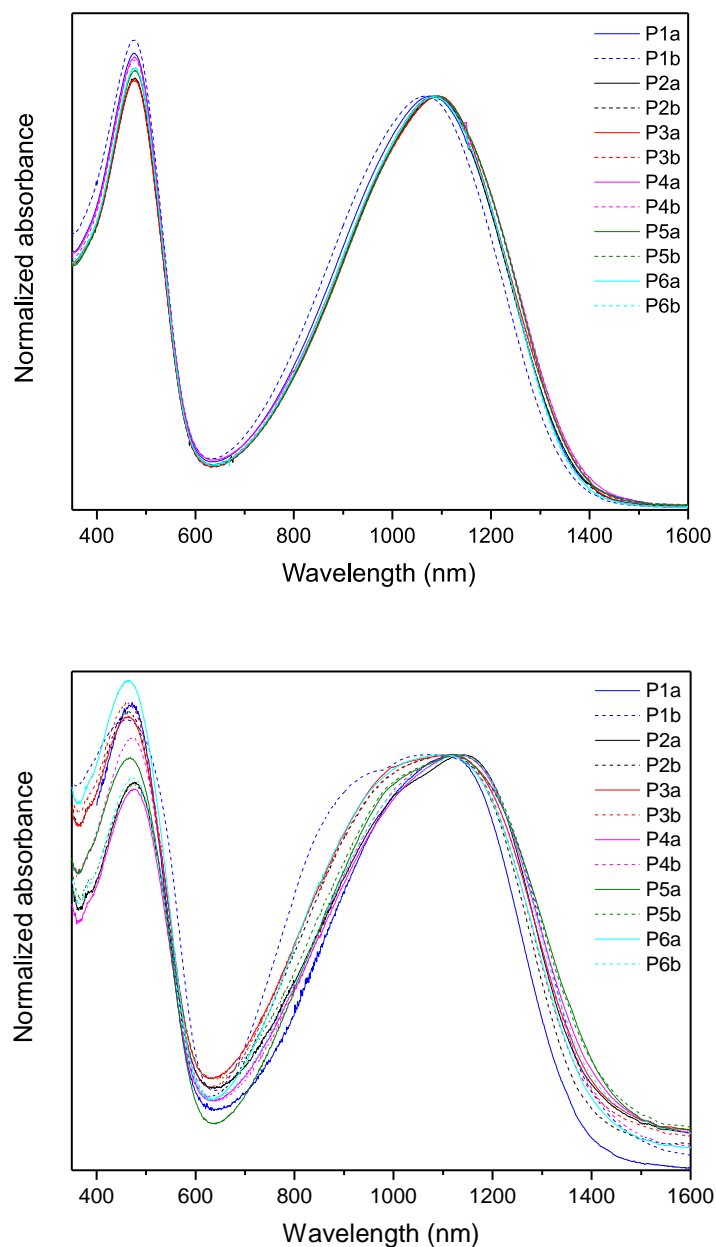


Figure 2: UV-VIS-NIR absorption spectra in chloroform solution (top) and in thin film (bottom) for the synthesized PTTQ(HD) polymer samples (a and b).

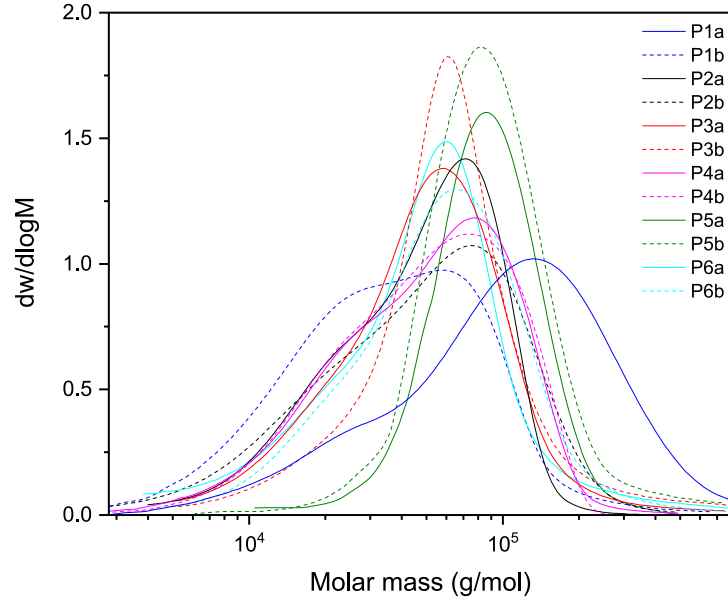


Figure 3: GPC profiles for the synthesized PTTQ(HD) polymer samples (a and b).

Since variations in polymer molar mass and the accompanying differences in microstructure and stacking tendency have a major influence on material processing and device performance, the synthesized polymers were evaluated in prototype OPDs. All devices were fabricated using an inverted architecture (ITO/ZnO/polymer:PC₇₁BM/MoO₃/Ag) and the previously optimized processing conditions.²⁴ Since the specific detectivity (D^*) is the main figure of merit for photodetectors, this parameter was used for comparison between the different polymer samples. The specific detectivity was determined at -2 V, where shot noise is assumed to have the main contribution to noise, via the equation

$$D^* = \frac{\text{EQE} \sqrt{q \Delta f} \lambda}{hc \sqrt{2J_D}},$$

with EQE the external quantum efficiency, q the elementary charge of an electron, Δf the frequency range, λ the incident wavelength, h Planck's constant, c the speed of light and J_D the dark current density. It is clear that D^* is influenced by both the EQE and the dark current, but the latter has a major influence as it can vary over several orders of magnitude. Therefore, both the EQE and the current-voltage (I - V) characteristics in darkness were investigated. The dark I - V curves, EQE spectra and resulting D^* values (vs wavelength, at -2 V bias) are depicted in Figure 4.

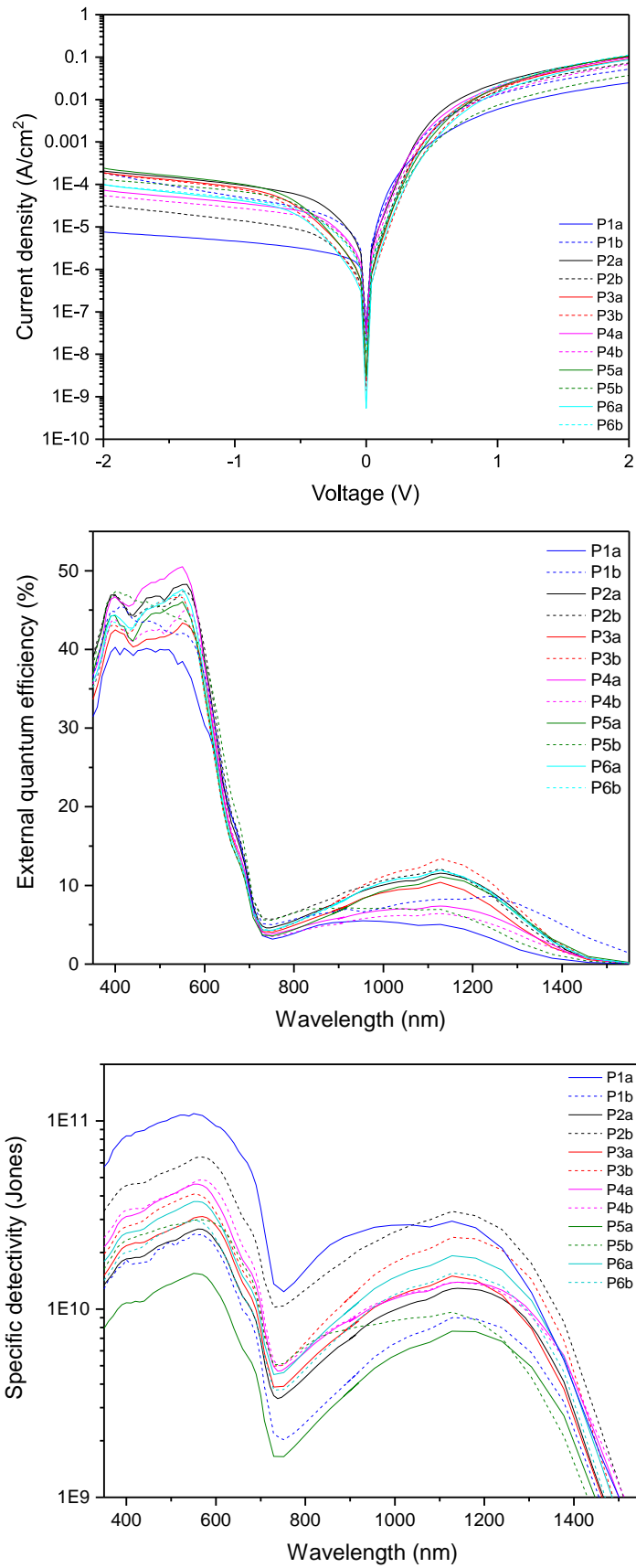


Figure 4: Current density-voltage curves under dark conditions (top), EQE spectra measured at -2 V (middle) and shot noise limited specific detectivities (vs wavelength) at -2 V bias (bottom) for the NIR-OPD devices based on PTTQ(HD).

Comparing device results, it can be seen that the flow polymers generally perform on the same level as the batch polymers (see also Figure S6). The device processing protocol was kept constant to keep the number of variables minimal. Upon individual processing optimization for the different polymer batches, even more similar results are expected. More important to note is the high consistency of the performance parameters for all flow samples, and especially the droplet flow samples (Figure 4). The batch samples (**P1**) have the largest average spread in D^* . The regular flow samples (**P2**) already show a smaller variation, but the droplet flow samples (**P3–P6**), yet again, have the smallest average difference. The higher degree of control offers a clear advantage in terms of consistency relative to batch chemistry.

In summary, this work illustrates the benefits of continuous droplet flow chemistry for the field of organic electronics. A droplet flow protocol has for the first time been developed for push-pull copolymer synthesis. Because of its resistance to precipitates and highly viscous solutions, droplet flow clearly enhances the scope of traditional flow chemistry. It also facilitates the transfer from batch to flow, since changes to the reaction conditions are no longer required. Moreover, the two-phase character allows straightforward and consistent molar mass tuning, which clearly benefits the final device performance reproducibility. Polymers made by droplet flow outperform the materials synthesized using the traditional batch and flow methods in terms of consistency, while affording similar device performance. Additionally, droplet flow reactors are very suitable for screening purposes. Since a single droplet of a reaction mixture can be injected into the immiscible carrier fluid, only very small quantities of a material are required for reaction screening, which is hence very cost-effective. On the other hand, the system can easily be scaled up, allowing large-scale production. In general, this technique allows the preparation of highly uniform, qualitative materials, which is a crucial factor for both academic research and industry.

Supporting Information Available

Material synthesis (batch and flow) protocols, OPD fabrication and characterization details and illustrative MALDI-ToF mass spectra, as well as a short movie illustrating the droplet flow protocol, are provided as Supporting Information.

Acknowledgements

O.B. thanks Hasselt University for financial support. S.G. and F.V. acknowledge the Research Foundation – Flanders (FWO Vlaanderen) for granting them a PhD fellowship. P.V. is a postdoctoral fellow of the FWO Vlaanderen. W.M. and K.V. are grateful for project funding by the FWO (G0D0118N, G0B2718N and Hercules project GOH3816NAUHL). Hasselt University and IMOMEC have been partners in the SBO project MIRIS (Monolithic Infrared Image Sensors), supported by VLAIO (Vlaams Agentschap Innoveren en Ondernemen). The authors also thank Dr. Geert Pirotte for his contribution to this project.

References

- (1) Reis, M. H.; Leibfarth, F. A.; Pitet, L. M. Polymerizations in Continuous Flow: Recent Advances in the Synthesis of Diverse Polymeric Materials. *ACS Macro Lett.* **2020**, *9* (1), 123–133. <https://doi.org/10.1021/acsmacrolett.9b00933>.
- (2) Seyler, H.; Jones, D. J.; Holmes, A. B.; Wong, W. W. H. Continuous Flow Synthesis of Conjugated Polymers. *Chem. Commun.* **2012**, *48* (10), 1598–1600. <https://doi.org/10.1039/c1cc14315h>.
- (3) Grenier, F.; Aïch, B. R.; Lai, Y. Y.; Guérette, M.; Holmes, A. B.; Tao, Y.; Wong, W. W. H.; Leclerc, M. Electroactive and Photoactive Poly[Isoidigo-Alt-EDOT] Synthesized Using Direct (Hetero)Arylation Polymerization in Batch and in Continuous Flow. *Chem. Mater.* **2015**, *27* (6), 2137–2143. <https://doi.org/10.1021/acs.chemmater.5b00083>.
- (4) Helgesen, M.; Carlé, J. E.; Dos Reis Benatto, G. A.; Søndergaard, R. R.; Jørgensen, M.; Bundgaard, E.; Krebs, F. C. Making Ends Meet: Flow Synthesis as the Answer to Reproducible High-Performance Conjugated Polymers on the Scale That Roll-to-Roll Processing Demands. *Adv. Energy Mater.* **2015**, *5* (9), 1401996. <https://doi.org/10.1002/aenm.201401996>.
- (5) Gao, M.; Subbiah, J.; Geraghty, P. B.; Chen, M.; Purushothaman, B.; Chen, X.; Qin, T.; Vak, D.; Scholes, F. H.; Watkins, S. E.; Skidmore, M.; Wilson, G. J.; Holmes, A. B.; Jones, D. J.; Wong, W. W. H. Development of a High-Performance Donor-Acceptor Conjugated Polymer: Synergy in Materials and Device Optimization. *Chem. Mater.* **2016**, *28* (10), 3481–3487. <https://doi.org/10.1021/acs.chemmater.6b01194>.
- (6) Bannock, J. H.; Krishnadasan, S. H.; Nightingale, A. M.; Yau, C. P.; Khaw, K.; Burkitt, D.; Halls, J. J. M.; Heeney, M.; De Mello, J. C. Continuous Synthesis of Device-Grade Semiconducting Polymers in Droplet-Based Microreactors. *Adv. Funct. Mater.* **2013**, *23* (17), 2123–2129. <https://doi.org/10.1002/adfm.201203014>.
- (7) Bannock, J. H.; Xu, W.; Baïssas, T.; Heeney, M.; de Mello, J. C. Rapid Flow-Based Synthesis of Poly(3-Hexylthiophene) Using 2-Methyltetrahydrofuran as a Bio-Derived Reaction Solvent. *Eur. Polym. J.* **2016**, *80*, 240–246. <https://doi.org/10.1016/j.eurpolymj.2016.04.016>.
- (8) Pirotte, G.; Kesters, J.; Verstappen, P.; Govaerts, S.; Manca, J.; Lutsen, L.; Vanderzande, D.; Maes, W. Continuous Flow Polymer Synthesis toward Reproducible Large-Scale Production for Efficient Bulk Heterojunction Organic Solar Cells. *ChemSusChem* **2015**, *8* (19), 3228–3233. <https://doi.org/10.1002/cssc.201500850>.
- (9) Pirotte, G.; Agarkar, S.; Xu, B.; Zhang, J.; Lutsen, L.; Vanderzande, D.; Yan, H.; Pollet, P.; Reynolds, J. R.; Maes, W.; Marder, S. R. Molecular Weight Tuning of Low Bandgap Polymers by Continuous Flow Chemistry: Increasing the Applicability of PffBT4T for Organic Photovoltaics. *J. Mater. Chem. A* **2017**, *5* (34), 18166–18175. <https://doi.org/10.1039/c7ta05627c>.
- (10) Gobalasingham, N. S.; Carlé, J. E.; Krebs, F. C.; Thompson, B. C.; Bundgaard, E.; Helgesen, M. Conjugated Polymers Via Direct Arylation Polymerization in Continuous Flow: Minimizing the Cost and Batch-to-Batch Variations for High-Throughput Energy Conversion. *Macromol. Rapid Commun.* **2017**, *38* (22), 1700526. <https://doi.org/10.1002/marc.201700526>.
- (11) Pirotte, G.; Verstappen, P.; Vanderzande, P. D.; Maes, P. W. On the “True” Structure of Push-Pull Type Low Bandgap Polymers for Organic Electronics. *Adv. Electron. Mater.* **2018**, 1700481. <https://doi.org/10.1002/aelm.201700481>
- (12) Katsouras, A.; Gasparini, N.; Koulogiannis, C.; Spanos, M.; Ameri, T.; Brabec, C. J.; Chochos, C. L.; Avgeropoulos, A. Systematic Analysis of Polymer Molecular Weight Influence on the

- Organic Photovoltaic Performance. *Macromol. Rapid Commun.* **2015**, *36* (20), 1778–1797. <https://doi.org/10.1002/marc.201500398>.
- (13) Li, W.; Yang, L.; Tumbleston, J. R.; Yan, L.; Ade, H.; You, W. Controlling Molecular Weight of a High Efficiency Donor-Acceptor Conjugated Polymer and Understanding Its Significant Impact on Photovoltaic Properties. *Adv. Mater.* **2014**, *26* (26), 4456–4462. <https://doi.org/10.1002/adma.201305251>.
- (14) Xiao, Z.; Sun, K.; Subbiah, J.; Qin, T.; Lu, S.; Purushothaman, B.; Jones, D. J.; Holmes, A. B.; Wong, W. W. H. Effect of Molecular Weight on the Properties and Organic Solar Cell Device Performance of a Donor-Acceptor Conjugated Polymer. *Polym. Chem.* **2015**, *6* (12), 2312–2318. <https://doi.org/10.1039/c4py01631a>.
- (15) Vangerven, T.; Verstappen, P.; Drijkoningen, J.; Dierckx, W.; Himmelberger, S.; Salleo, A.; Vanderzande, D.; Maes, W.; Manca, J. V. Molar Mass versus Polymer Solar Cell Performance: Highlighting the Role of Homocouplings. *Chem. Mater.* **2015**, *27* (10), 3726–3732. <https://doi.org/10.1021/acs.chemmater.5b00939>.
- (16) Spoltore, D.; Vangerven, T.; Verstappen, P.; Piersimoni, F.; Bertho, S.; Vandewal, K.; Van Den Brande, N.; Defour, M.; Van Mele, B.; De Sio, A.; Parisi, J.; Lutsen, L.; Vanderzande, D.; Maes, W.; Manca, J. V. Effect of Molecular Weight on Morphology and Photovoltaic Properties in P3HT:PCBM Solar Cells. *Org. Electron.* **2015**, *21*, 160–170. <https://doi.org/10.1016/j.orgel.2015.02.017>.
- (17) Hartman, R. L.; McMullen, J. P.; Jensen, K. F. Deciding Whether to Go with the Flow: Evaluating the Merits of Flow Reactors for Synthesis. *Angew. Chem. Int. Ed.* **2011**, *50* (33), 7502–7519. <https://doi.org/10.1002/anie.201004637>.
- (18) Li, Q.; Guo, Y.; Liu, Y. Exploration of Near-Infrared Organic Photodetectors. *Chem. Mater.* **2019**, *31* (17), 6359–6379. <https://doi.org/10.1021/acs.chemmater.9b00966>.
- (19) Chen, C. H.; Wang, Y.; Michinobu, T.; Chang, S. W.; Chiu, Y. C.; Ke, C. Y.; Liou, G. S. Donor-Acceptor Effect of Carbazole-Based Conjugated Polymer Electrets on Photoresponsive Flash Organic Field-Effect Transistor Memories. *ACS Appl. Mater. Interfaces* **2020**, *12* (5), 6144–6150. <https://doi.org/10.1021/acsami.9b20960>.
- (20) Murto, P.; Minotto, A.; Zampetti, A.; Xu, X.; Andersson, M. R.; Cacialli, F.; Wang, E. Triazolobenzothiadiazole-Based Copolymers for Polymer Light-Emitting Diodes: Pure Near-Infrared Emission via Optimized Energy and Charge Transfer. *Adv. Opt. Mater.* **2016**, *4* (12), 2068–2076. <https://doi.org/10.1002/adom.201600483>.
- (21) Rivnay, J.; Inal, S.; Salleo, A.; Owens, R. M.; Berggren, M.; Malliaras, G. G. Organic Electrochemical Transistors. *Nat. Rev. Mater.* **2018**, *3*, 17086. <https://doi.org/10.1038/natrevmats.2017.86>.
- (22) Kielar, M.; Dhez, O.; Pecastaings, G.; Curutchet, A.; Hirsch, L. Long-Term Stable Organic Photodetectors with Ultra Low Dark Currents for High Detectivity Applications. *Sci. Rep.* **2016**, *6* (December), 39201. <https://doi.org/10.1038/srep39201>.
- (23) Verstraeten, F.; Gielen, S.; Verstappen, P.; Kesters, J.; Georgitzikis, E.; Raymakers, J.; Cheyns, D.; Malinowski, P.; Daenen, M.; Lutsen, L.; Vandewal, K.; Maes, W. Near-Infrared Organic Photodetectors Based on Bay-Annulated Indigo Showing Broadband Absorption and High Detectivities up to 1.1 μm . *J. Mater. Chem. C* **2018**, *6* (43), 11645–11650. <https://doi.org/10.1039/c8tc04164d>.
- (24) Verstraeten, F.; Gielen, S.; Verstappen, P.; Raymakers, J.; Penxten, H.; Lutsen, L.; Vandewal, K.;

- Maes, W. Efficient and Readily Tuneable Near-Infrared Photodetection up to 1500 nm Enabled by Thiadiazoloquinoxaline-Based Push-Pull Type Conjugated Polymers. *J. Mater. Chem. C* **2020**, *8* (29), 10098–10103. <https://doi.org/10.1039/D0TC01435D>.
- (25) Newman, S. G.; Jensen, K. F. The Role of Flow in Green Chemistry and Engineering. *Green Chem.* **2013**, *15* (6), 1456–1472. <https://doi.org/10.1039/c3gc40374b>.
- (26) Wiles, C.; Watts, P. Continuous Flow Reactors: A Perspective. *Green Chem.* **2012**, *14* (1), 38–54. <https://doi.org/10.1039/c1gc16022b>.
- (27) Jas, G.; Kirschning, A. Continuous Flow Techniques in Organic Synthesis. *Chem. - A Eur. J.* **2003**, *9* (23), 5708–5723. <https://doi.org/10.1002/chem.200305212>.
- (28) Wegner, J.; Ceylan, S.; Kirschning, A. Flow Chemistry - A Key Enabling Technology for (Multistep) Organic Synthesis. *Adv. Synth. Catal.* **2012**, *354* (1), 17–57. <https://doi.org/10.1002/adsc.201100584>.
- (29) Watts, P.; Haswell, S. J. The Application of Micro Reactors for Organic Synthesis. *Chem. Soc. Rev.* **2005**, *34* (3), 235–246. <https://doi.org/10.1039/b313866f>.
- (30) Reis, M. H.; Varner, T. P.; Leibfarth, F. A. The Influence of Residence Time Distribution on Continuous-Flow Polymerization. *Macromolecules* **2019**, *52* (9), 3551–3557. <https://doi.org/10.1021/acs.macromol.9b00454>.